P-ISSN 2586-9000
E-ISSN 2586-9027
Homepage : https://tci-thaijo.org/index.php/SciTechAsia
Science & Technology Asia
Vol. 28 No.2 April - June 2023
Page: [1-8]
Original research article

Annealing Effect on Structural and Morphological Properties of MnS/MnO_2 Nanocomposite

M. Nirmala*, B. Kavitha, S. Anupriya, J. Sree Sudha

Department of Physics, Sri GVG Visalakshi College for Women, Tamilnadu 642128, India

Received 2 February 2021; Received in revised form 17 August 2022
Accepted 14 December 2022; Available online 14 June 2023

ABSTRACT

Nanocomposite of MnS/MnO_2 has been prepared by a modest Hydrothermal method. The heating effect on MnS/MnO_2 Nano composites was studied by various characterization techniques. The crystalline nature of the as prepared and annealed MnS/MnO_2 Nanocomposite was analyzed using X-ray diffraction. Surface morphological analysis was carried out using a Scanning Electron Microscope. EDAX analysis was taken to confirm the composition of Nanocomposite. The functional groups were confirmed by using Fourier transform Spectroscopy. The result suggests that prepared MnS/MnO_2 Nano composite is very suitable for super capacitor applications.

Keywords: Fourier transform infrared spectroscopy; Hydrothermal; Nanocomposite; SEM; XRD

1. Introduction

Perfect and renewable energy resources are urgently needed to deal with environmental pollution and the end of fossil fuels [1, 2]. Electrochemical energy storage and energy innovations, such as super capacitors, lithium-ion batteries, fuel cells and solar cells are considered as future renewable energy sources due to their insignificant impacts on the environment [3, 4]. The development of these energy systems with high energy and power outputs, and long lifetimes is needed and noteworthy for applications in many vital zones such as electric vehicles and engineering equipment, etc. [5]. Amongst the various energy storage systems, super capacitors have a lot of appeal due to their high-power density, large capacitance, low cost and long cycle life compared to traditional batteries and conventional capacitors [6, 7]. Several metal oxides such as TiO_2, MnO_2, NiO, RuO_2, Co_2O_3, and MoO_3 have been used for super capacitor electrode congregation [8-13].

***Corresponding author:** saicharan.kumar16@gmail.com

RuO_2 shows an unexpected electrochemical property with high explicit capacitance due to its large number of oxidation states. However, the high cost and toxicity of RuO_2 limit the commercialization of RuO_2 electrode-based supercapacitors [14]. Conversely, MnO_2-based electrodes have attracted great interest due to their low toxicity, low cost, and better electrochemical property. For the past two decades, several research investigations have been conducted using MnO_2-based composites as super capacitor electrodes. Although MnO_2-based electrodes reveal high specific capacitance, the specific capacitance value radically decreases at strong current regimes due to high electrical resistivity, which reduces the performance as well the cycle constancy of the super capacitor [15].

To enhance the performance of MnO_2 electrode, various transition metals/metal oxides and nanocarbon materials such as, TiO2, ZnO, Co, Cu, carbon nanotubes, graphene activated carbon and etc. were merged [16-18]. Still, the performance of MnO_2 nanomaterials requires further improvement. Recently, metal sulfides were accepted as a promising group of electrically active materials for super capacitor electrode fabrication. For instance, MnS, MoS_2, NiS, RuS, WS_2 and CoS were extensively probed for energy storage applications [19, 20] Among them, MnS revealed remarkable specific capacitance due to its high conductivity (3.2×10^{-3} Scm^{-1}) and structural faces.

MnS is well known to have a strong redox reaction and stores the energy by the non-faradaic procedure. The layered lamellar nanostructure of MnS offers high ionic permeation and intercalation-deintercalation, which improves the electrochemical stability of super capacitor. In addition, Manganese disulfide is inexpensive and eco-friendly, with high thermal steadiness, compared with other metal sulfides. For instance, Teng et al. reported the synthesis of MnS nanocrystals for supercapacitor application and achieved a specific capacitance value of 573.9 Fg^{-1} at a current density of 0.5 Ag^{-1} [21] Unfortunately, the phase transfer, poor rate and lower cycle performance of MnS limit the everyday applications [22] Thus, the performance of pure MnS-based super capacitors does not compete with other metal oxides/sulfides and still needs to be improved.

To resolve this problem, many studies have been devoted to the preparation of various metal sulfide mixed/doped MnS nanocomposites. Recently, the hydrothermal process has opened a successful route for the synthesis of advanced inorganic materials that are tough or impossible to obtain by high temperature solid state reactions [23, 24]. The main benefit of such a soft solution process is to bring the preparation of metastable phases or to diminish significantly the reaction temperature and successively the sintering effects.

2. Materials and Methods

The MnS/MnO_2 nanocomposite was synthesized by a low temperature hydrothermal method. Analytical grade precursors were purchased and used for the preparation of MnS/MnO_2 nanocomposite. 1M of $KMnO_4$ was dissolved in 20ml of distilled water and stirred for 30 minutes. 1M of manganese chloride tetra hydrate and 1M of Na_2S were added to the $KMnO_4$ solution while stirring and continued for 2 hours. The mixture was then transferred to a Teflon coated autoclave and dried for 6 hours at 100ºC and then washed with distilled water several times. The mixture was then dried in a hot air oven for 6 hours at 100ºC and grained for 2 hours. The prepared MnS/MnO_2 nanocomposite was annealed at two different temperatures of 150ºC and 250ºC, respectively, using muffle furnace for 1 hour.

X-ray diffraction analysis was carried out using a powder X-ray diffractometer (Schimadzu model: XRD 6000) with Cu-Kα radiation of 0.154187 nm wavelength to inspect the formation, crystalline behavior and the quality of synthesized MnS/MnO_2 nanocomposite. The scanning was done in the region of 2θ from 30º to 80º. The grain size of MnS/MnO_2 nanocomposite was calculated by the Debye-Scherer equation. The surface morphology and particle size of synthesized MnS/MnO_2 nanocomposite were investigated by JEOL, JSM-67001(Scanning Electronic Microscope). The chemical composition in the MnS/MnO_2 nanocom-posite was determined by using a Philips XL 20 energy dispersive X-ray (EDX) analysis. Fourier Transform Infrared spectra study was used to identify the presence of functional groups. FT-IR spectra were measured by a JASCO FTIR spectrometer having a resolution of 1 cm^{-1} in the wavelength range 500-4000 cm^{-1}.

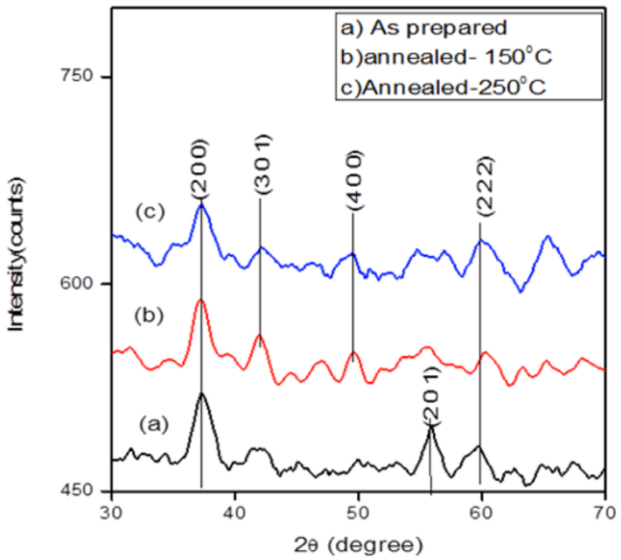

Fig.1. XRD pattern of MnS/MnO_2 Nanocomposite.

Table 1. XRD parameters of MnS/MnO_2 Nanocomposite.

Sample	**2θ (degree)**	**(h k l)**	**Crystalline Size**
MnS/MnO2	34.4	111	26.71
	37.3	200	8.11
	55.8	201	14.47
	59.9	222	20.27
avg			17
MnS/MnO_2 (150 ºC)	37.19	200	12.97
	41.84	301	23.98
	49.53	400	18.10
	60.14	222	34.08
avg			22
MnS/MnO_2 (250 ºC)	37.32	200	11.77
	42.11	301	21.21
	50.27	400	27.83
	59.86	222	22.05
avg			21

3. Results and Discussion

3.1 Structural analysis (XRD)

The structural appearances of prepared MnS/MnO_2 nanocomposites were studied using XRD analysis. Fig. 1 shows the XRD pattern of as prepared MnS/MnO_2 nanocomposite (see Table 1). MnS/MnO_2 nanocomposite exhibit diffraction peaks at angles of 34º4', 37º3', 55º8', and 59º9' and their corresponding (h k l) planes were indexed to the values of (1 1 1), (2 0 0), (2 0 1), and (2 2 2) [25]. Also, for the annealed MnS/MnO_2 nanocomposite, the diffraction peaks were observed at 37º1', 41º8', 49º5', 60º1' for 150ºC and 37º3', 42º1', 50º2', 59º8' for 250ºC, respectively, and their corresponding (h k l) planes were (2 0 0), (3 0 1), (4 0 0) and (2 2 2) [26]. The observed XRD pattern matched with JCPDS No. 01-076-6012. The crystalline size based on X-ray diffraction is determined with the help of Debye-Scherrer's formula as $D = k\lambda / \beta \cos\theta$. The average crystalline size was found to be 17 nm for as-prepared MnS/MnO_2 nanocomposite, 22 nm and 21 nm for MnS/MnO_2 nanocomposite at 150ºC and 250ºC, respectively. Crystallite sizes increased after annealing the samples due to atomistic rearrangement and relieving of residual stress of lattice. The peaks in the XRD pattern will broaden as the crystalline size decreases [27]. The XRD pattern revealed that the peak broadening would happen when the annealing temperature increases, which is due to change in growth rate between the different crystallographic planes. No peaks were observed for Sodium and Sulfur compounds in the XRD pattern. Peak intensity also was found to be decreased for annealed MnS/MnO_2 nanocomposite.

3.2 Scanning electron microscope (SEM)

The surface morphology of the synthesized MnS/MnO_2 nanocomposite was studied with the help of SEM. Fig. 2 displays the SEM image of the MnS/MnO_2 nanocomposite annealed at 150ºC. This figure evidently reveals that the MnS/MnO_2-150ºC nanocomposite has coral like structure in the 1µm range.

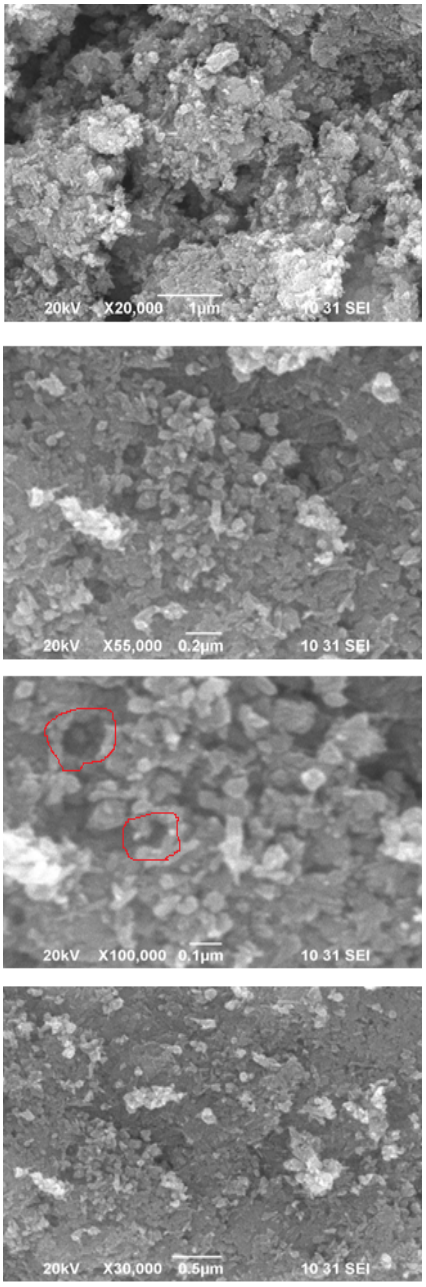

Fig. 2. SEM images of MnS/MnO_2 Nanocomposite.

3.3 Energy dispersive analysis of x-ray (EDAX)

The chemical compositions of the prepared MnS/MnO_2 nanocomposite were studied with the help of EDAX. Fig. 3 shows the EDAX spectrum of the MnS/MnO_2 nanocomposite annealed at 150ºC. Only Manganese, Oxide and Sulphur peaks were observed in the MnS/MnO_2 nanocomposite. The observed weight percentage values were near to the standard theoretical weight percentage values. The weight percentage values are shown in below.

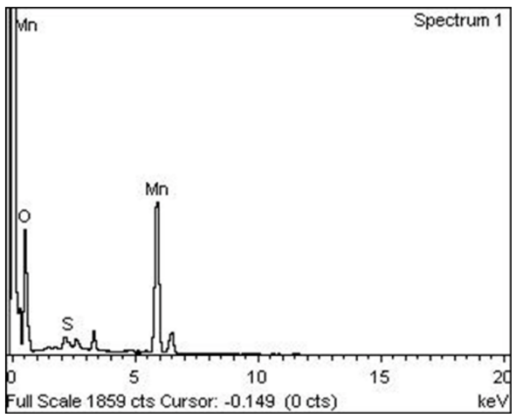

Fig. 3. EDX Spectrum of MnS/MnO_2 Nanocomposite annealed at 150ºC.

Table 2. EDX spectrum confirmed the presence of representative elements in the nanocomposite.

Table 2. Compositional Analysis of MnS/MnO_2 Nanocomposite annealed at 150ºC.

Elements	Weight %	Atomic %
Mn	34.92	64.78
S	0.16	0.15
O	64.92	35.07
Total	100	100

3.4 Fourier transform infra-red spectroscopy (FTIR)

The characteristic peaks of MnS/MnO_2 nanocomposites were examined by Fourier Transform Infrared Spectrometer (FTIR) in the range of 4000-500 cm^{-1}. The most characteristics peaks observed in the synthesized MnS/MnO_2 nanocomposite are shown in Fig. 4. The band located at 700.5 cm^{-1} corresponds to the vibrational stretching of MnO and MnS vibrations. The additional bands observed at approximately 1226 cm^{-1} and 1210 cm^{-1} were assigned to the sulfide source in MnS indicating the coordination between Mn atoms in MnS [28]. The broad absorption peaks in the range 1627cm^{-1},1624 cm^{-1} and 1375 cm^{-1} were assigned to the C=O stretching modes due to the absorption of carbon dioxide. The bands at 3379 cm^{-1}, 3370 cm^{-1} 1740 cm^{-1}, 1741 cm^{-1} and 1743 cm^{-1} correspond to the existence of O-H vibrating modes.

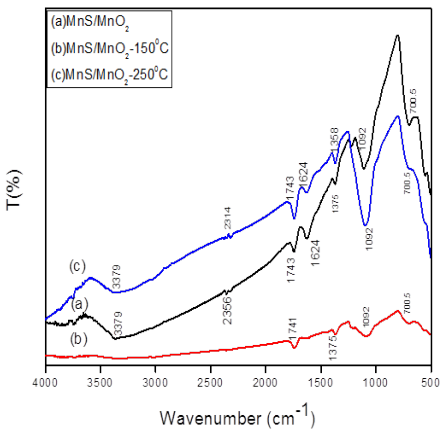

Fig. 4. FTIR Spectra of MnS/MnO_2 Nanocomposite.

4. Conclusion

The MnS/MnO_2 nanocomposite was synthesized by Hydro- thermal method. The synthesized MnS/MnO2 nanocomposite was annealed at 150 ºC and 250 ºC, respectively. The MnS/MnO_2 nanocomposites were characterized by XRD, FTIR, SEM and EDAX analysis. The XRD

analysis revealed that the crystalline size 'D' was increased with annealing temperature. The average crystalline size was found to be 17 nm for as-prepared MnS/MnO_2 nanocomposite,22 nm and 21 nm for 150ºC and 250ºC annealing temperatures. The observed band at 700.5 cm^{-1} resembled the vibrational stretching of MnO and MnS from the FTIR studies. The surface morphology of the MnS/MnO_2 nanocomposite displayed the coral like structure and there was no cluster due to annealing. EDAX analysis confirmed the occurrence of Mn, O and S compounds in the MnS/MnO_2 nanocomposite. It has been seen that significant improvement of supercapacitors can be achieved by using optimized MnO_2/MnS nano composite electro active materials.

Acknowledgement

The authors are grateful to the Secretary, Principal and Head of the Department of Physics, Sri G.V.G Visalakshi College for Women, Udumalpet for their excellent encouragement and support. The work was supported by DBT Star College Scheme and Department of Science and Technology (DST).

References

[1] Dong L, Chen Z, Yang D, Lu H. Hierarchically structured Graphene-based Supercapacitor Electrodes. RSC Adv. 2013;3:21183-91.

[2] Miller J, Simon P. Electrochemical Capacitors for Energy Management. Science. 2008:321: 651-52.

[3] Zhang L.L, Zhao X.S. Carbon-based materials as Supercapacitor Electrodes Chem. Soc. Rev. 2009;38: 2520-31.

[4] Li X, Wei B. Supercapacitors based on nanostructured carbon. Nano Energy. 2013;2: 159-73.

[5] Simon P, Gogotsi Y. Materials for electrochemical capacitors. Nat. Mater. 2008;7: 845-54.

[6] Zhang J, Jiang Li H, Zhao XS. A high-performance asymmetric Supercapacitor fabricated with Graphene-based Electrodes. Energy Environ. Sci., 2011;4: 4009-15.

[7] Zhou Z, Wu XF. Graphene-beaded Carbon Nanofibers for use in Supercapacitor Electrodes: Synthesis and Electrochemical Characterization. J. Power Sources. 2013;222: 410-6.

[8] Lu Xihong, Gongming Wang, Teng Zhai, Minghao Yu, Jiayong Gan, Yexiang Ton, Yat Li. Hydrogenated TiO2 nanotube arrays for supercapacitors. Nano letters 2012;12(3): 1690-6.

[9] Zhu Shijin, Li Li, Jiabin Liu, Hongtao Wan, Tian Wan, Yuxin Zhang, Lili Zhang, Rodney S Ruoff. Fan Dong. Structural directed growth of ultrathin parallel Birnessite on β-MnO_2 for high-performance asymmetric Supercapacitors. ACS nano 2018;12(2):1033-42.

[10] Hu Bingling, Xiaoyun Qin, Abdullah M Asiri, Khalid A Alamry, Abdulrahman O Al-Youbi, Xuping Sun. Fabrication of $Ni(OH)_2$ Nanoflakes array on Ni foam as a binder-free electrode material for high performance Supercapacitors. Electrochimica Acta.2013;107: 339-42.

[11] Liu Tongchang, Pell WG, Conway BE. Self-discharge and potential recovery phenomena at thermally and Electrochemically prepared RuO_2 Supercapacitor Electrodes. Electrochimica Acta. 1997;42: 3541-52.

[12] Yu Zhan Jun, Ying Dai, Wen Chen. Synthesis of CO_2O_4 Microspheres by Hydrothermal-Precipitation for Electrochemical Supercapacitors. In Advanced Materials Research. 2009;66; 280-3.

[13] Peng Huihua, Chuan Jing, Jie Chen, Deyi Jiang, Xiaoying Liu, Biqin Dong, Fan Dong, Shaochun Li, Yuxin Zhang. Crystal structure of Nickel Manganese-layered double Hydroxide@ Cobaltosic oxides on Nickel foam towards high-performance Supercapacitors. CrystEngComm. 2019;21(3): 470-7.

[14] Lu Wen-Jing, Shi-Ze Huang, Ling Miao, Ming-Xian Liu, Da-Zhang Zhu, Liang-Chun Li, Hui Duan, Zi-Jie Xu, Li-Hua Gan. Synthesis of MnO_2/N-doped Ultramicroporous Carbon Nanospheres for high-performance Supercapacitor Electrodes. Chinese Chemical Letters. 2017;28(6): 1324-9.

[15] Śliwak Agata, Adam Moyseowicz. Grażyna Gryglewicz. Hydrothermal-assisted synthesis of an Iron Nitride–Carbon composite as a novel Electrode material for Supercapacitors. Journal of Materials Chemistry A. 2017;5: 5680-4.

[16] Lu Xihong, Minghao Yu, Gongming Wang, Teng Zhai, Shilei Xie, Yichuan Ling, Yexiang Tong, Yat Li. H-TiO2@MnO2//H-TiO2@C Core–Shell Nanowires for High Performance and Flexible Asymmetric Supercapacitors. Advanced materials. 2013; 25(2): 267-72.

[17] Yu Mingpeng, Hongtao Sun, Xiang Sun, Fengyuan Lu, Gongkai Wang, Tao Hu, Hong Qiu, Jie Lian. Hierarchical Al-doped and Hydrogenated ZnO nanowire@MnO_2 Ultrathin Nanosheet core/shell arrays for high-performance Supercapacitor Electrode. Int. J. Electrochem. Sci. (2013);8: 2313-29.

[18] Tang Chuan-Lin, Xiao Wei, Yan-Mei Jiang, Xue-Yan Wu, Li-Na Han, Kai-Xue Wang, Jie-Sheng Chen. Cobalt-doped MnO_2 Hierarchical Yolk–shell spheres with improved Supercapacitive Performance. The Journal of Physical Chemistry C. 2015;119(16): 8465-71.

[19] Pujari RB, Lokhande AC, Yadav AA, Kim JH, Lokhande CD. Synthesis of MnS Microfibers for high performance flexible Supercapacitors. Materials & Design.2016;108: 510-7.

[20] Hu Bingling, Xiaoyun Qin, Abdullah M Asiri, Khalid A Alamry, Abdulrahman O Al-Youbi, Xuping Sun. Synthesis of porous tubular C/MOS_2 Nanocomposites and their Application as a Novel Electrode Material for Supercapacitors with excellent cycling Stability. Electrochimica Acta. 2013;100: 24-8.

[21] Chen Teng, Yongfu Tang, Yuqing Qiao, Zhangyu Liu, Wenfeng Guo, Jianzheng Song, Shichun Mu, Shengxue Yu, Yufeng Zhao, Faming Gao. All-Solid-State high performance asymmetric Supercapacitors based on novel MnS Nanocrystal and activated Carbon materials. Scientific reports. 2016;6: 23289-98.

[22] Zhang Guanggao, Menglai Kong, Yadong Yao, Lu Long, Minglei Yan, Xiaoming Liao, Guangfu Yin, Zhongbing Huang, Abdullah M. Asiri, Xuping Sun. One-pot synthesis of γ-MnS/reduced Graphene Oxide with Enhanced Performance for aqueous Asymmetric Supercapacitors. Nano-technology. 2017;28(6): 065402-414.

[23] Yoshimura M. Importance of soft solution processing for Advanced Inorganic Materials. J. Mater. Res. 1998;13: 796-02.

[24] Demazeau G. Solvothermal processes: A Route to the Stabilization of New Materials J. Mater. Chem. 1999; 9: 15-8.

[25] Cao Yong, Ming-sen Zheng, Senrong Cai, Xiaodong Lin, Cheng Yang, Weiqiang Hu, Quan-feng Dong. Carbon embedded Alpha MnO2 Graphene Nanosheet Composite: A Bifunctional Catalyst for high Performance Lithium Oxygen Batteries. Journal of Materials Chemistry A. 2014;44:18736-741.

[26] Huang Xiao, Zhinguo Zhang. Huan Li.Yingyuan Zhao. Hongxia Wang. Tingil Ma.Novel fabrication of Ni3S2/MnS Composite as high Performance Supercapacitor Electrode. Journal of Alloys and Compounds. 2017;722:662-68.

[27] Muhammed Shafi, Chandra Bose A. Impact of crystalline defects and size on X-ray line broadening: A phenomenological approach for Tetragonal SnO_2 Nanocrystals. AIP Advances. 2015;5: 057137.

[28] Rajesh Rajagopal, Kwang-Sun Ryu. Synthesis of MnO_2 Nanostructures with MnS Deposits for High Performance Supercapacitor Electrodes. New J. Chem. 2019;43:12987-3000.